Journal of
*Marine Science and Engineering*

MDPI

*Article*

# An Evaluation of Treatment Effectiveness for Reclaimed Coral Sand Foundation in the South China Sea

**Ting Yao [1] and Wei Li [2,*]**

[1] Sate Key Laboratory of Geomechanics and Geotechnical Engineering, Institute of Rock and Soil Mechanics, Chinese Academy of Sciences, Wuhan 430071, China; tyao@whrsm.ac.cn
[2] Faculty of Engineering, China University of Geosciences, Wuhan 430074, China
* Correspondence: liwei35@cug.edu.cn

**Abstract:** Mega land reclamation projects have been carried out on the coral reefs in the South China Sea. Coral sand was used as a backfill material through hydraulic filling, with fill heights ranging from 6 to 10 m. To enhance foundation stability, vibro-flotation and impact rolling have been employed. However, the uneven distribution of coral sand, irregular particle shape, lower single-particle strength, and paucity of engineering cases for reference have posed challenges in evaluating the effectiveness of these foundation treatments. In this study, the effectiveness of vibro-flotation and impact rolling on the densification and bearing capacity of coral sand foundations has been investigated. In situ tests, including the plate load test, California Bearing Ratio (CBR) test, density measurements, dynamic penetration test (DPT), and settlement monitoring, were conducted at four distinct zones: an untreated zone, a vibro-flotation zone at a 5 m depth, a vibro-flotation zone at a 10 m depth, and an impact rolling zone. The findings suggest that coral sand exhibits promising characteristics for foundation construction. Seepage and self-weight consolidation following land reclamation formation significantly enhance the compaction degree of the coral sand foundation, thereby meeting the requirements for areas with lower bearing capacity demands. Both vibro-flotation and impact rolling techniques could significantly enhance the foundation-bearing capacity, with marginal differences between them. Since the machinery is simple and construction speed is quick, the impact rolling method is considered to be the most efficient for the treatment of coral sand foundation. The DPT results suggest that the reinforcement effect of both vibro-flotation and impact rolling on the deep foundation is not as substantial as the surface layers. This study provides valuable insights into optimizing foundation treatments for land reclamation projects on the coral reefs.

**Keywords:** land reclamation; hydraulic filling; coral sand; foundation treatment; vibro-flotation; impact rolling



**Citation:** Yao, T.; Li, W. An Evaluation of Treatment Effectiveness for Reclaimed Coral Sand Foundation in the South China Sea. *J. Mar. Sci. Eng.* **2023**, *11*, 2288. https://doi.org/10.3390/jmse11122288

Academic Editor: Tom Spencer

Received: 24 October 2023
Revised: 26 November 2023
Accepted: 29 November 2023
Published: 1 December 2023



## 1. Introduction

Coral reefs are predominantly distributed in tropical oceans between N 30° and S 30° and are formed by *Scleractinia*, algae, and various marine organisms through biological processes [1]. In response to the growing demand for space and resources, extensive land reclamation projects have been undertaken on the coral reefs of the South China Sea. This involves excavating coral sand and debris from lagoons and reef flats using cutter suction dredgers, followed by the pumping of these materials through the pipeline onto the reef flat [2]. Through this method, the construction cost can be reduced and the construction period can be shortened significantly [3,4].

Coral sand is primarily composed of calcium carbonate, with distinct differences from terrigenous sediments formed through physical, biochemical, and chemical processes [5]. It has been observed that coral sands exhibit rich intra-particle pores, irregular particle shapes, and high susceptibility to breakage [6–8]. However, they possess higher peak and critical state friction angles, along with higher liquefaction resistance compared to quartz sand [9–13]. The authors of the *Hydraulic Fill Manual for Dredging and Reclamation Works* [14] designated coral sand as a specialized filling material, emphasizing its advantageous engineering performance and the potential for enhanced strength and stiffness over time due to particle bonding.

Traditionally, hydraulic-filled marine soils are characterized by their low-density and high-water content, as well as their void ratio, rendering them unsuitable as backfill material due to their low bearing capacity, high compressibility, and prolonged consolidation time [15,16]. Foundation treatment becomes imperative to enhance the bearing capacity of hydraulic-filled soils. However, there is currently no consensus on reinforcement methods for coral sand foundations. In the land reclamation areas within coral reefs, the filling layer is typically thicker than 5 m [4,17]. The vibro-flotation method has traditionally been employed to densify deeply buried hydraulic filling materials due to its commendable reinforcement effects; however, it is time-consuming and economically inefficient. Sand foundations are also commonly reinforced via impact rolling [18], which combines impact and rolling functions, providing a fast construction speed and cost-effectiveness [19]. Nevertheless, it falls short of meeting the requirements for deep subgrade reinforcement. Dynamic compaction, which utilizes instantaneous impact loads, has been utilized to compact soil, reduce soil compressibility, and enhance soil strength [20,21]. However, Ke et al. [22] declared that a coral sand foundation treated using dynamic compaction remains susceptible to liquefaction and that the reinforcement effect of dynamic compaction on the subgrade below the groundwater is minimal. Following on-site observation, it was found that the compaction degree of hydraulic-filled coral sand foundations nearly meets the criteria for use as the foundation for airports or other engineering structures with a straightforward foundation treatment [17].

In the case of quality control for a hydraulic-filled coral sand foundation, Van Impe et al. [23] highlighted that both the discharge methods of the dredgers, i.e., rainbowing or tilting, and ground improvement techniques, including dynamic compaction, rolling compaction, or vibro-compaction, can induce different initial stress an-isotropy and stress histories in coral sand. Therefore, in practical applications reinforcing hydraulic-filled coral sand foundation, relying solely on the tip resistance-relative density ($q_c$-$D_r$) relationship is insufficient and should be abandoned. Giretti et al. [24] also pointed out that empirical correlations developed with silica sands cannot be applied in the presence of crushable materials such as carbonate sands. Furthermore, Giretti et al. [25] performed a cone penetration test (CPT) calibration using a centrifuge model with supplementary large-scale calibration chamber tests, and a relationship between the $q_c$ of CPT and state parameter was established, which serves as a pivotal benchmark for evaluating the reinforcement efficacy., Wang et al. [17] emphasized that the hydraulic-filled coral soils, in the land reclamation projects on the coral reefs in the South China Sea, exhibited uneven particle size distributions, ranging from silt-sized particles to blocks. Notably, the CPT sensors often faced damage when encountering these blocks, leading to test failures and inaccurate results. Consequently, the more resilient and cost-effective approach of utilizing the dynamic penetration test (DPT) was chosen to assess the density and bearing capacity of the coral soil foundation. Wang et al. [17] also found that there is an approximately linear relationship between the bearing capacity of the coral soil foundation and the blow count of DPT ($N_{63.5}$). Based on the above considerations, the DPT was also adopted for evaluating the performance of the current hydraulic-filled coral sand foundation.

In this study, the reclaimed foundation has a thick layer of hydraulic-filled coral sand, typically ranging from 6 to 10 m. It is crucial to carry out in situ experimental research on the treatment effectiveness of the coral sand foundation as it helps in exploring the optimal treatment scheme and technical construction parameters of coral sand foundations, allowing us to determine the quality control standard of foundation treatments and ensure the quality of the subsequent construction. The reclamation of reef islands in the South China Sea is mainly for the construction of airports. The requirement for an airport foundation bearing capacity is around 200 kPa [26], and a shallow foundation is normally enough to bear the overlying structures. Since previous experiences were limited and the construction time was short, two common methods of treating inland foundations, vibro-flotation and impact rolling, were employed to treat the hydraulic-filled coral sand foundation. After treatment, the plate load test, California Bearing Ratio (CBR) test, density measuring, and settlement monitoring were performed to evaluate the compaction degree, bearing capacity, and settlement of the surface layer, which is the main bearing layer; moreover, dynamic penetration test (DPT) was adopted for assessing the bearing capacity and compactness of deeper foundation soils.

## 2. Site Conditions

The study area is on a reef island in the South China Sea (Figure 1a), and the stratigraphy of the studied reef island, as depicted in Figure 1b, comprises six distinct layers. The uppermost layer represents the hydraulic filling layer, primarily consisting of uncemented coral soils with particle sizes ranging from silt to blocks. The second layer is the original reef flat, which is covered by a layer of beach rocks that extend to approximately 2 m in thickness, cemented by algae and laying about 1–2 m below sea level. Below the reef flat, the third to fifth layers consist of lightly cemented coral debris, predominantly composed of coral soil, shell remnants, and reef blocks. The sixth layer comprises the cemented reef limestone stratum. Comprehensive topographical and subsurface information about the reef island can be found in Sun et al. [27]. Figure 2 shows the hydraulic filling process for creating foundations for the construction of infrastructures, mainly including airport runways, drainage works, pipe gallery construction, oil tanks, and associated buildings. In this method, sedimentary coral sands near the reef platform are dredged by a large-scale cutter suction dredger and pumped through pipelines along with seawater onto the reef platform. Through the self-weight consolidation of the coral sand, excess water drains away, and a certain stable elevation is achieved.

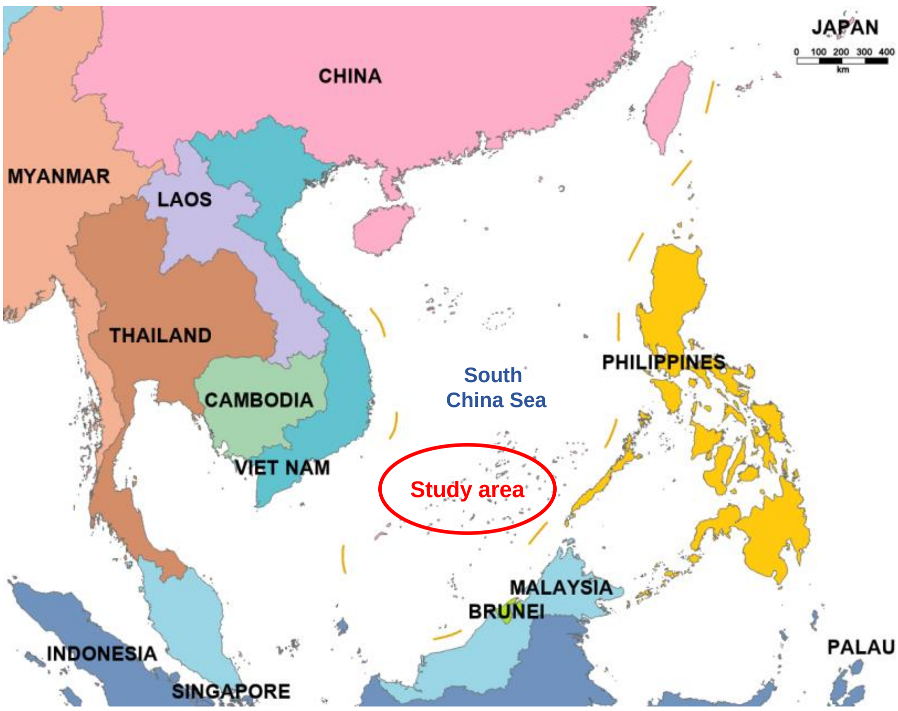


(**a**)

**Figure 1.** *Cont.*

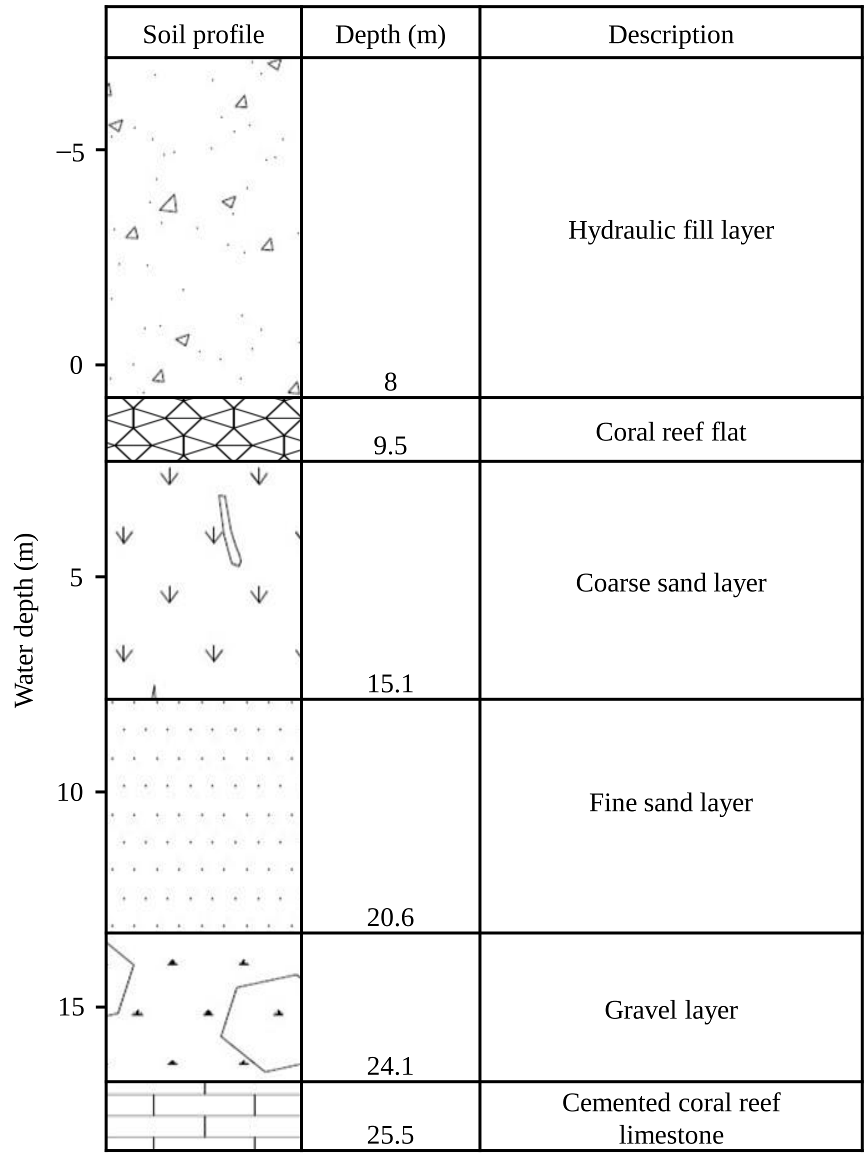


(**b**)

**Figure 1.** (**a**) Location of study area; (**b**) profile of the stratigraphy of the studied reef island.

**Figure 2.** Formation of coral sand foundation.

The hydraulic-filled coral sand is mainly formed through the accumulation of the skeletal remains of marine organisms like shells and corals. The soil particles often exhibit irregular branching, spindle-like, flaky, and blocky shapes, among others, with a higher content of branching and spindle-like particles. Coarser particles often show more irregular shapes with numerous intra-particle pores, while the finer particles have relatively regular shapes but still contain a significant number of intra and surface pores, as shown in Figure 3, which is also observed in Yao and Li [12]. Sieving tests were performed on five sets of coral sand samples collected from the surface of the hydraulic fill, where particles coarser than 4.75 mm (about 2–4%) were removed. The grading curves of the coral sand samples are presented in Figure 4. It can be seen that the particles with sizes ranging from 0.3 to 0.6 mm have the highest content, accounting for approximately 28.8% of the total mass. The median particle size ($d_{50}$) is around 0.44 to 0.68 mm, the coefficient of uniformity ($C_u$) falls within the range from 4.00 to 5.62, and the coefficient of curvature ($C_c$) is in the range from 0.85 to 1.05. According to the ASTM [28] D2487, among the five samples, 1, 4, and 5 are well graded, while 2 and 3 are poorly graded, indicating that there is a certain degree of variability in the distribution of soil materials at the site. The fundamental physical properties of the coral sands are listed in Table 1. The minimum dry density of the coral sand samples was determined according to ASTM [29] D4254. In the case of measuring the maximum dry density, the vibration hammering method was used to avoid significant particle damage [30]. Three parallel tests were performed for each measurement to obtain an average value.

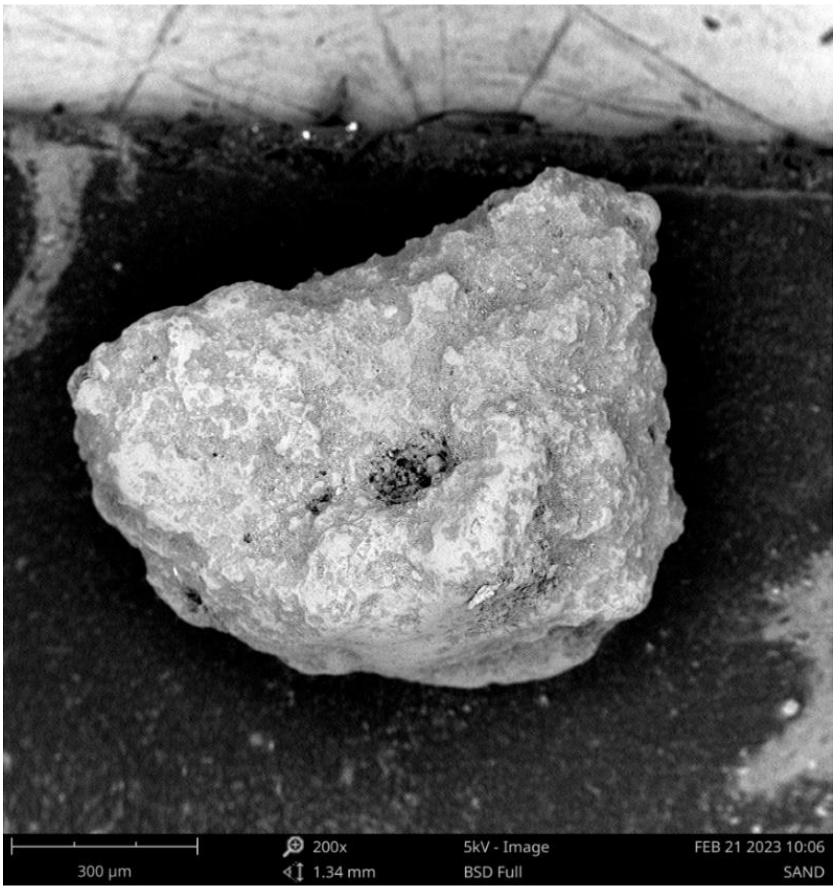


(**a**)

**Figure 3.** *Cont.*

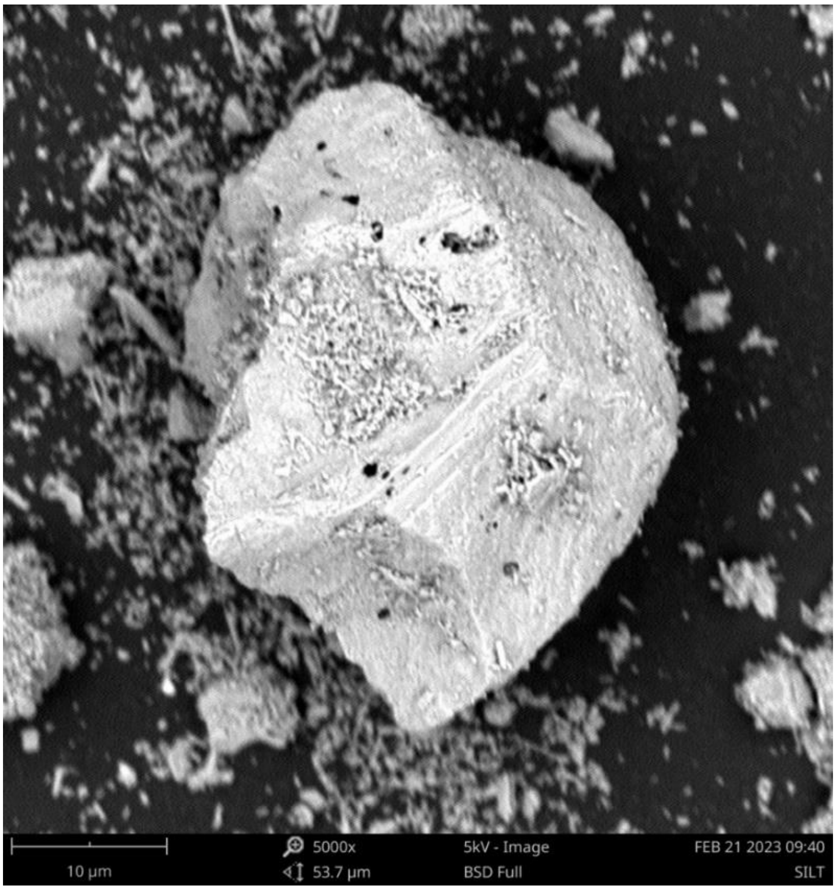


(**b**)

**Figure 3.** SEM images of coral sand: (**a**) coarse particle; (**b**) fine particle.

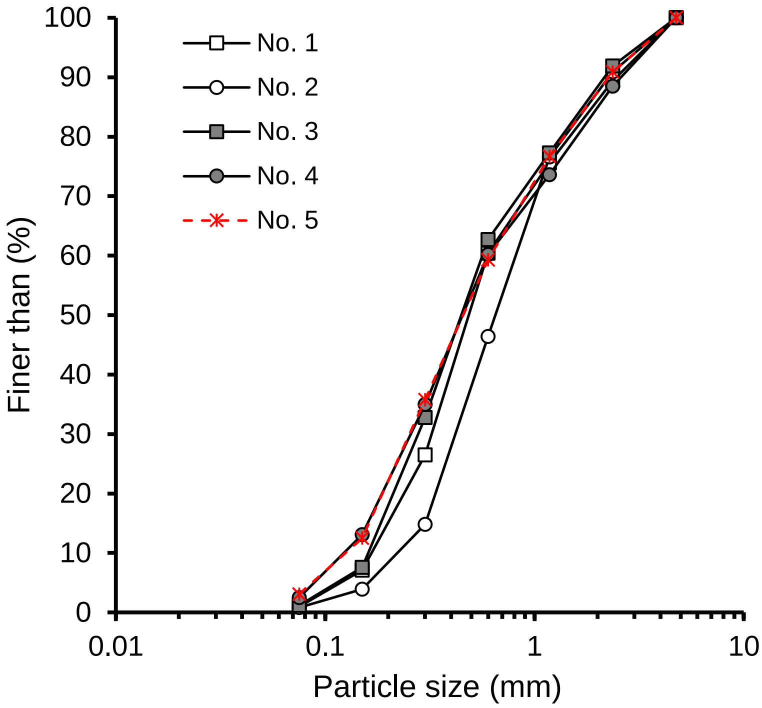


**Figure 4.** Particle size distribution curves of the hydraulic-filled coral sand.

**Table 1.** Fundamental physical properties of the calcareous soils.

| $G_s$ | $e_{max}$ | $e_{min}$ | $w_i$ (%) | $\rho_{di}$ (g/cm$^3$) | $\rho_{d,max}$ (g/cm$^3$) | $\rho_{d,min}$ (g/cm$^3$) |
|---|---|---|---|---|---|---|
| 2.8 | 1.31 | 0.69 | 16.3–21.2 | 1.43–1.48 | 1.66 | 1.21 |

Note: $G_s$, specific gravity; $e_{max}$, maximum void ratio; $e_{min}$, minimum void ratio; $w_i$, water content after self-weight consolidation; $\rho_{di}$, dry density after self-weight consolidation; $\rho_{d,max}$, maximum dry density; $\rho_{d,min}$, minimum dry density.

## 3. Foundation Treatment Schemes

The study area was divided into four experimental zones, including one zone (A1) without post-filling treatment, two zones (A2 and A3) with vibro-flotation treatment, and one zone (A4) with impact rolling treatment. The purpose was to assess the treatment effects of coral sand foundations under different treatment techniques. The thickness of the hydraulic-filled coral sand layer in each experimental zone was approximately 7 to 8 m, and the depth of groundwater was around 2 m. The specific dimensions and layout of each zone are shown in Figure 5.

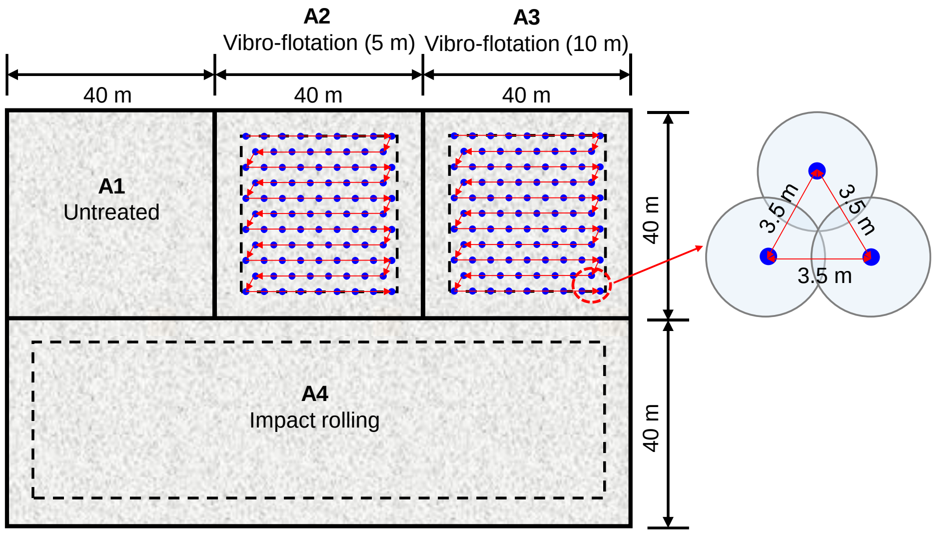


**Figure 5.** Dimensions and layout of each experimental zone.

During on-site implementation, hydraulic filling was first performed to create the initial onshore foundation. After the filling was completed, the site was left for one month to allow seepage and drainage. Once the seepage and drainage processes were stable and met the conditions for foundation treatment, the on-site foundation treatment was initiated. The treatment methods for each experimental zone were as follows:

(1) Untreated Zone A1: After the formation of the coral sand foundation through hydraulic filling, no further foundation treatment was conducted. The improvement of the foundation relied solely on self-weight consolidation.

(2) Vibro-flotation Zones A2 and A3: A 180 kW dynamic vibrator was used for the foundation treatment. The zones were divided into A2 and A3 based on different treatment depths, with compaction depths of 5 m and 10 m, respectively. The vibro-flotation points were arranged in an equilateral triangle and the distance between two treatment points was 3.5 m. According to in situ observation, it was found that the effective vibration zone of the 180 kW dynamic vibrator has a diameter of about 4 m, beyond which the soil density was almost unaffected. The layouts of the treatment points as well as the construction sequence can be observed in Figure 5.

(3) Impact Rolling Zone A4: A 25 kJ triangular roller was used to impact and roll the surface layer of the hydraulic-filled coral sand. In total, 20 rolling passes were performed for the treatment.

During the treatment, to prevent the mutual interference of seepage effects in different experimental zones after foundation treatment and to expedite the drainage and self-weight consolidation process, a 2 m deep drainage trench was excavated around each experimental zone after the completion of filling. Additionally, a 5 m wide untreated platform was left around each experimental zone during the treatment process.

## 4. On-Site Evaluation Tests

After the foundation treatment was completed, a series of evaluation tests were conducted on site, including a plate load test, California Bearing Ratio (CBR) test, soil density measurement, and dynamic penetration test (DPT), to identify the extent of the increase in the foundation density and bearing capacity, assess the deformation characteristics, and analyze the reinforcement depth. Finally, the monitoring data of the on-site settlement of the hydraulic-filled coral sand foundation were discussed.

### *4.1. Normal Shallow Plate Load Test*

The shallow plate load test is a direct means of measuring the bearing capacity and deformation modulus of the foundation and typically involves recording the foundation settlement under incremental loading, which could reflect the foundation's resistance to deformation [31]. The maximum load applied is generally twice the design load of the foundation. In this study, the maximum design load is 300 kPa; therefore, a maximum load of 600 kPa was employed. A square steel plate with sides of 1000 mm and a thickness of 50 mm was used as the loading plate. Counterweights in conjunction with a high-pressure hydraulic pump were employed to apply the load incrementally, and the displacement of the load plate at various time points and under different pressures was recorded using a dial gauge. A curve illustrating displacement as a function of pressure was plotted, i.e., the p–s curve. According to GB 50007-2011 [31], when there is a proportional limit on the p–s curve, the load value corresponding to the proportional limit is taken as the characteristic value of the bearing capacity; however, when the ultimate load is less than the load value of the corresponding proportional limit, half of the ultimate load should be taken as the characteristic value of the bearing capacity. The deformation modulus is calculated according to the following equation [32]:

$$E = I_0\left(1-\mu^2\right)\frac{pb}{s} \tag{1}$$

where $E$ represents the deformation modulus of the foundation; $p$ denotes the vertical stress in the linear segment of the p–s curve; s corresponds to the settlement associated with $p$; $b$ is the side length or diameter of the bearing plate; $I_0$ stands for the shape factor of the bearing plate (0.886 for a square plate); $\mu$ is the Poisson's ratio, and 0.3 is adopted for coral sands according to He et al. [33]. The shallow plate load tests were performed immediately after completing the foundation treatment and leveling the surface. For each experimental zone, three points near the center were randomly tested.

### *4.2. Plate Load Test for Determining the Modulus of the Subgrade Reaction*

As a design parameter for pavement structures, the modulus of the subgrade reaction is typically used to determine the strength of the airport pavement foundation, reflecting the foundation's resistance to deformation. The modulus of the subgrade reaction can be determined by a specialized plate load test. In this test, an increasing load was applied to a bearing plate with a diameter of 760 mm. Deformation values under varying loads were measured to obtain a p–s curve. Based on Winkler's model, the modulus of the subgrade reaction can be calculated using the following equation [34]:

$$K_u = \frac{p_B}{0.00127} \tag{2}$$

where $K_u$ represents the modulus of the subgrade reaction and $p_B$ denotes the vertical stress corresponding to a settlement of 1.27 mm. After the treatment, plate load tests were conducted at three random points on the leveled surface in each experimental zone.

### *4.3. CBR Test*

The CBR test is mainly for determining the stiffness of road subgrades. A penetration rod with a 50 mm metal cylinder was pressed into the subgrade at a rate of 1 mm/min. The pressure at a specific depth (usually 2.5 mm) was compared to the standard pressure for that penetration depth, which gave the measured *CBR* value for the subgrade [35]. The formula for calculating the *CBR* value is as shown below:

$$CBR = \frac{P_1}{P_0} \times 100\% \tag{3}$$

where $P_1$ is the measured vertical stress at the corresponding penetration depth and $P_0$ is the standard pressure for a 2.5 mm penetration depth (7 MPa). Similar to the plate load tests, in situ CBR tests were carried out at three randomly chosen locations within each experimental zone.

### *4.4. Soil Density Measurement*

The compaction degree is one of the most important indicators for the quality control of the soil foundation, which refers to the ratio of the dry density of the compacted material to its maximum dry density. Only through adequate compaction of the foundation can the safety and stability of the upper structure construction be ensured. The density of coral sand was determined using the sand-filling method [35]. In each experimental zone, the density of the surface layer of the coral sand foundation (0–1.0 m) was assessed at 8 randomly chosen positions.

### *4.5. Dynamic Penetration Test*

The dynamic penetration (DPT) test is a quick and cost-effective method for indirectly assessing the bearing capacity and compactness of deeper foundation soils. In this study, a heavy dynamic penetration test was employed using a 63.5 kg heavy hammer dropped freely from a fixed height of 76 cm to drive the probe rod into the soil. The number of blows required for the probe rod to penetrate 10 cm was recorded as $N_{63.5}$, thus obtaining DPT values at different depths [36]. The DPT tests were performed at nine randomly selected positions within each experimental zone after the foundation treatment. Considering the hydraulic filling depth on the reef island ranging from 5 to 10 m, the DPT examination depth was set as 6 m, with $N_{63.5}$ values recorded every 10 cm of penetration, commencing at a depth of 0.5 m.

### *4.6. Settlement Monitoring*

The elevation of each experimental zone was measured before and after the treatment to calculate the construction settlement. After the treatment, three surface settlement markers were buried in each zone to observe the post-construction settlement. For the untreated zone, settlement markers were set just after the reclaimed land formation.

## 5. Results and Discussion

### *5.1. Bearing Capacity and Deformation Modulus*

The representative p–s curves of the four experimental zones are shown in Figure 6a. It can be observed that, except for the A1 zone, there are no obvious inflection points on the p–s curves for the other zones. While on the site, it was found that, even when the tests reached their maximum loading of 600 kPa, there was no significant lateral extrusion of coral sand or a sudden increase in the settlement around the bearing plate for the A2, A3, and A4 zones. This suggests that the characteristic value of the bearing capacity must be at least 300 kPa for the three zones. Analyzing the p–s curve of the A1 zone, an inflection point appears at a load of 375 kPa, and a significant lateral extrusion of coral sand occurred when the load reached 450 kPa, indicating the onset of soil failure. This might be related to the particle breakage of the coral sand. Therefore, the load just before failure, 375 kPa, is taken as the ultimate load, and half of the ultimate load, 187.5 kPa, is considered the characteristic value of the bearing capacity of the A1 zone.

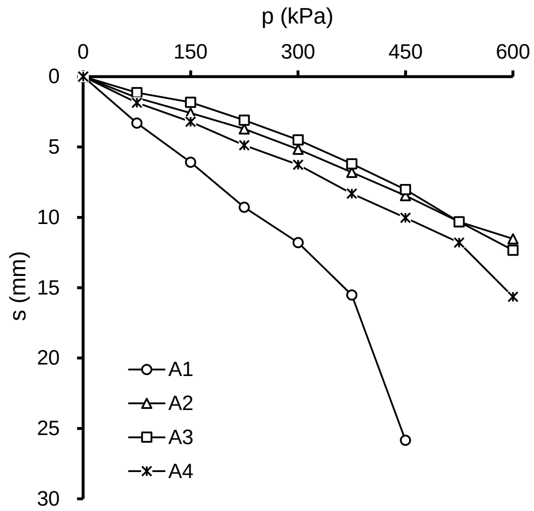


(**a**)

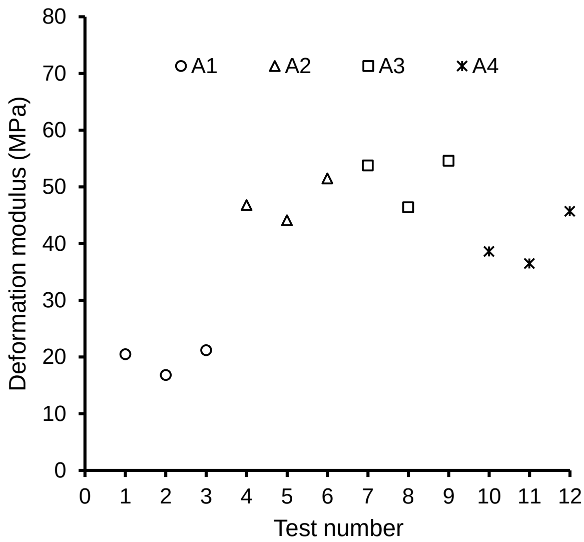


(**b**)

**Figure 6.** Shallow plate load testing results: (**a**) p–s curve; (**b**) deformation modulus.

It can be seen that the untreated coral sand foundation already has a relatively high bearing capacity that can meet the requirements of some light buildings and structures. At the same time, according to the p–s curves of the A2 and A3 zones, their differences are minimal, with the foundation bearing capacity and deformation modulus varying within the same range, indicating that there is no need to further extend the treatment depth to 10 m in vibro-flotation. The p–s curve of the A4 zone lies only slightly below those of A2 and A3, which suggests that surface impact rolling could effectively improve the bearing capacity of the coral sand foundation.

The deformation moduli of the four experimental zones, with three testing data for each zone, are shown in Figure 6b. It can be seen that the deformation modulus of the A1 zone is around 20 MPa, which is higher than common untreated terrestrial sands [37,38]. For the A4 zone, after the impact rolling treatment, the deformation modulus increases to about 40 MPa, essentially double that of the untreated zone. Firstly, this is because the soil particles rearrange and the void ratio reduces under the impact. Secondly, the impact force causes significant particle breakage, especially in the surface layer, further filling voids and increasing the degree of compaction. In contrast, although the deformation modulus of the A2 and A3 zones increases further under the vibro-flotation compaction treatment, the increase is marginal in comparison to the A2 zone.

### *5.2. Modulus of Subgrade Reaction*

The representative p–s curves of the four experimental zones for measuring the modulus of the subgrade reaction are shown in Figure 7a. It can be observed that, for the A1 zone without treatment, the vertical stress when the bearing plate settlement reaches 1.27 mm is 56 kPa. Therefore, the modulus of the subgrade reaction for the A1 zone is determined to be 44.0 MN/m$^3$. The value is relatively high and can essentially meet the design requirements for the clay and silt subgrades of an airport runway [34]. This indicates that seepage consolidation has a certain compaction effect on the coral sand foundation. Similarly, the modulus of the subgrade reaction for the A2, A3, and A4 zones after vibro-flotation and impact rolling treatments are found to be 91.8 MN/m$^3$, 97.2 MN/m$^3$, and 78.5 MN/m$^3$, respectively. The modulus of subgrade reaction after impact rolling increases by nearly a factor of two compared to the untreated state. The foundation capacity essentially meets the design requirements for the coarse-grained soil subgrades of an airport runway [34].

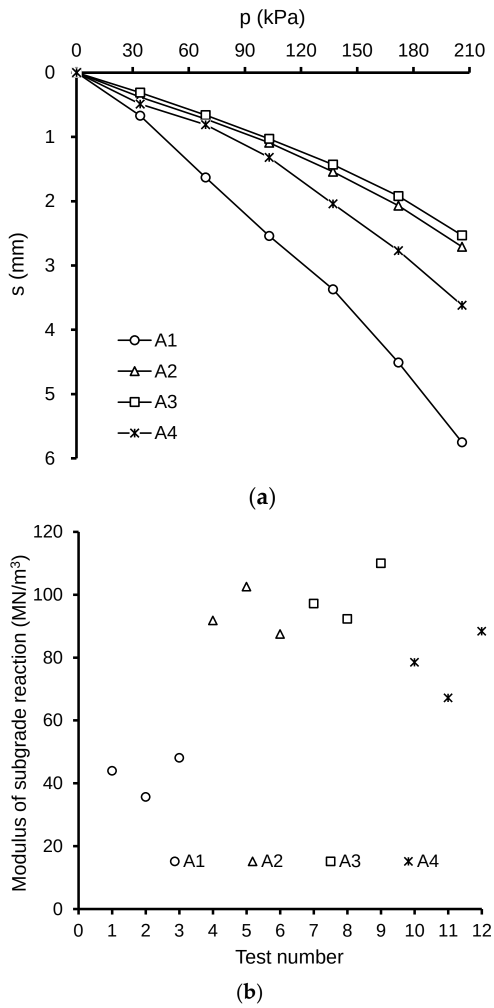


**Figure 7.** Modulus of subgrade reaction testing results: (**a**) p–s curve; (**b**) modulus of subgrade reaction.

The moduli of the subgrade reaction of the four experimental zones, with three testing data for each zone, are shown in Figure 7b. The average modulus of subgrade reaction for the A1, A2, A3, and A4 zones was found to be 42.6 MN/m$^3$, 94.0 MN/m$^3$, 99.8 MN/m$^3$, and 78 MN/m$^3$, respectively, indicating that the overall trend remains consistent with those described above.

### 5.3. CBR Value

The p–s curves from the representative location of each experimental zone are presented in Figure 8a. For the untreated A1 zone, the vertical stress at a penetration depth of 2.5 mm was 1092 kPa, and the corresponding CBR value was 15.6%. In accordance with AASHTO [39] T 193, a CBR value of 16% suggests that the soil may have a moderate-to-fair bearing capacity. The CBR values for the three treated zones are 66.5%, 66.0%, and 53.8%, respectively, indicating a significant improvement in the bearing capacity after vibro-flotation or impact rolling. Although the CBRs of the vibro-flotation-treated zones surpass those of impact rolling, considering the soil variability, both treatment methods are considered to be efficient.

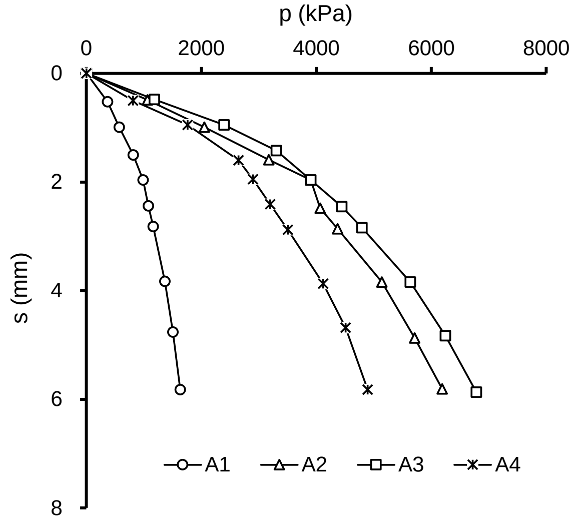


(**a**)

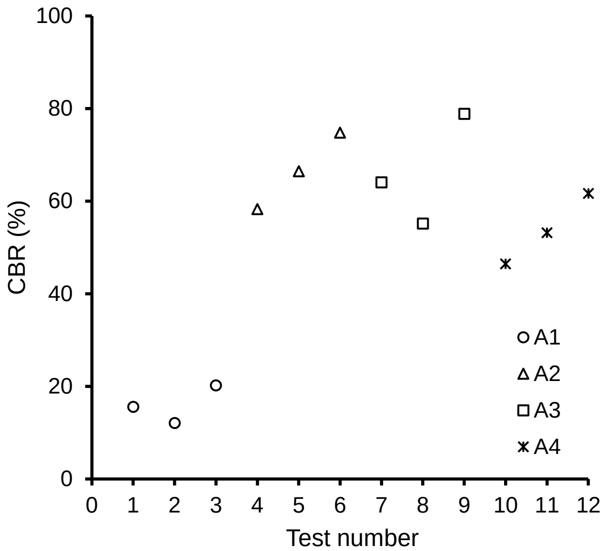


(**b**)

**Figure 8.** CBR testing results: (**a**) p–s curve; (**b**) CBR value.

A more detailed analysis of the CBR values for different experimental zones is shown in Figure 8b, where slightly scattered results could be observed within each experimental zone. Notably, the CBRs for the three tested positions within the untreated zone A1 consistently exceed 15%, with one reaching as high as 20%. This signifies that the stiffness of the hydraulic-filled coral sand foundation is already high enough for airport runway construction. Much higher CBR values are observed in the treated areas, which can be attributed to the substantial impact of both the vibro-flotation and impact rolling treatments on particle rearrangement and breakage, resulting in a much denser structure [4].

### 5.4. Soil Compactness

In each area, eight positions were randomly selected for the density measurement. The compaction degree of the hydraulic filling coral soils before and after treatment was determined by comparing the field-measured dry density, obtained through the sand replacement method, with the maximum dry unit weight of the coral sand achieved using the vibration hammering method (1.66 g/cm$^3$). The corresponding compaction degree for each point is summarized in Figure 9. The results show that the compaction degree within the A1 zone, which did not undergo any treatment, ranged from 86% to 90%, with a mean value of approximately 88% after hydraulic filling and self-weight consolidation. This suggests that the compaction degree of the hydraulic-filled coral sand foundation complies with the design requirements for areas with lower bearing capacity demands [34]. Following vibro-flotation and impact rolling treatment, due to the breakage of coarser coral sand particles, the voids are further filled. As a result, the compaction degree in the treated areas increases from 93% to 96%, essentially meeting the design requirements for airport construction [34]. The difference in enhancement between vibro-flotation and impact rolling, as seen in the comparison of the compaction degree, is negligible, with the difference in average values being less than 1%.

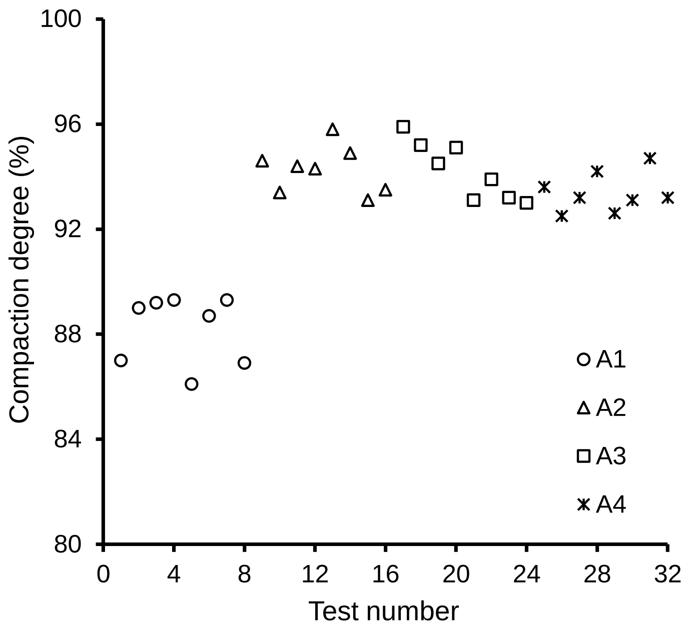


**Figure 9.** Compaction degree of the surface coral sand in each experimental zone.

Additionally, a comprehensive examination of the compaction degree was conducted at different depths and time intervals in a specific location within the A1 zone. This investigation aimed to understand the effects of seepage and self-weight consolidation on the densification of the coral sand. The evaluation spanned time periods of 1 week, 2 weeks, and 2 months following the reclaimed land formation. Figure 10 illustrates the compaction degree at this specific site. The data reveal a notable enhancement in the density of the coral sand ground after increased time following hydraulic filling, particularly during the first week. Subsequently, it stabilizes at around 14 days. Notably, one month later, the compaction degree within the top 1.0 m of the soil reaches 88.6%, aligning with the data shown in Figure 9. A comparison of the soil compaction degree at different depths indicates that the compactness improves with increasing burial depth, reaching as high as 90% within the 2.0–3.0 m range, and, in some instances, increasing up to 94%. This meets the essential requirement for airport subgrade quality. Self-weight consolidation plays a significant role in the densification of hydraulic-filled materials. Additionally, the relatively faster seepage velocity and the facilitated movement of finer particles within inter-particle voids are a consequence of the irregular particle shape of coral sand [40,41]. Both factors contribute to the densification of the coral sand.

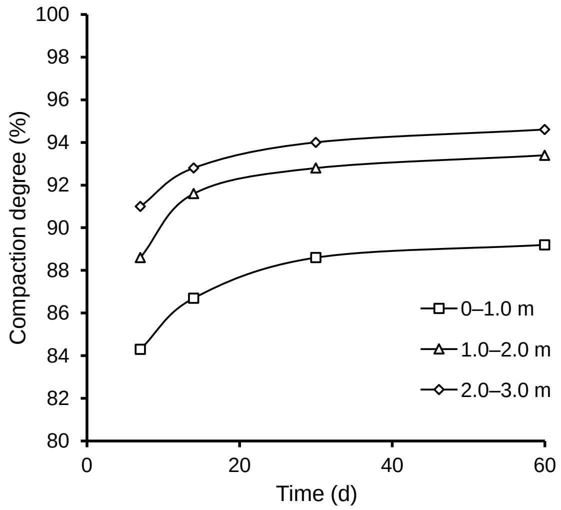


**Figure 10.** Compaction degree of the coral sand in the untreated zone at different depths and time intervals.

*5.5. DPT Result*

The test data for the four representative positions within each experimental zone in terms of the $N_{63.5}$ against depth are displayed in Figure 11. In the untreated A1 zone, the $N_{63.5}$ ranges from 5 to 12 within a 6 m depth. The scatteredness is mainly due to the uneven structure of the coral sand caused by the hydraulic filling process [42], with the maximum value having been found at a depth of 1.5–2.0 m. Beyond a depth of 3 m, the $N_{63.5}$ decreases due to the influence of groundwater. After foundation treatment, $N_{63.5}$ is generally greater than 10, with a maximum value of 23, indicating a significant improvement in foundation compactness. The most pronounced increase in $N_{63.5}$ occurs after vibro-flotation at a depth of 1–3 m. However, for foundation depths exceeding 3 m, the increase in $N_{63.5}$ is considerably less, suggesting that the reinforcement effect of both vibro-flotation and impact rolling on the deep foundation is not as substantial as the surface layers.

In each area, nine positions were randomly selected for the DPT evaluation. Figure 12 presents the average $N_{63.5}$ along the foundation depth for each test position. In the untreated area, the mean values of the $N_{63.5}$ range from approximately 7 to 11. After vibro-flotation treatments at depths of 5 m and 10 m, the $N_{63.5}$ values increase significantly, falling within the range from 14 to 24. However, the difference between the two tested zones within the depth of 6 m is not significant. In the impact rolling zone, the mean $N_{63.5}$ values increase to a range from 12 to 20. According to Wang et al. [17], when the $N_{63.5}$ of the coral sand foundation exceeds 10, it indicates a compaction degree higher than 85% and a bearing capacity greater than 500 kPa. In summary, the effectiveness of impact rolling meets the requirement for infrastructure construction.

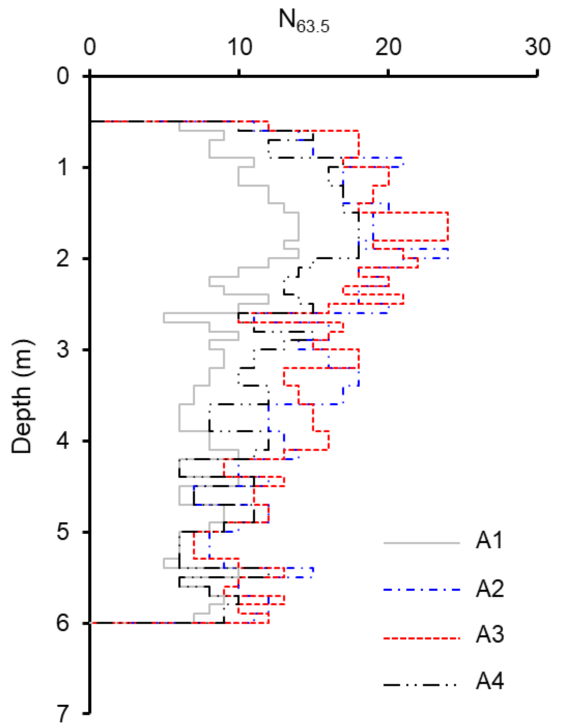


**Figure 11.** $N_{63.5}$ against depths of representative positions within each experimental zone.

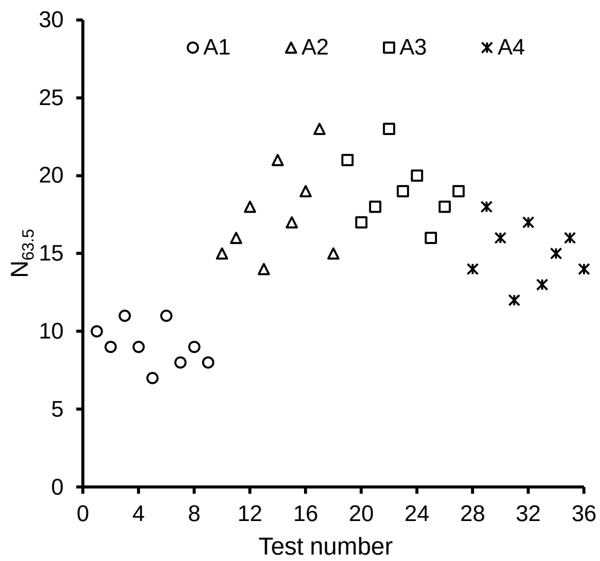


**Figure 12.** Average $N_{63.5}$ along the foundation depth for each test position.

### *5.6. Settlement Analysis*

The settlement of the untreated A1 zone over time is shown in Figure 13. It is evident that the coral sand foundation experiences significant settlement over time, and the settlement rate initially increases rapidly. As the drainage process continues, the settlement gradually stabilizes, reaching a relatively stable state after one month, with a maximum settlement of approximately 30 cm. As pointed out by Wang et al. [41], the coral sand particles are porous and have an angular shape, resulting in higher permeability than common terrigenous sand and rapid self-weight consolidation characteristics.

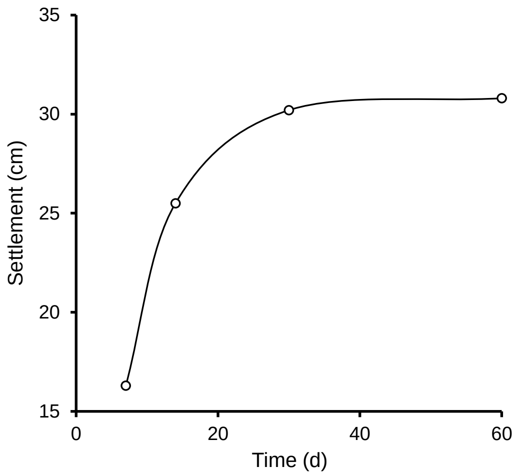


**Figure 13.** Settlement of the untreated A1 zone over time.

The additional construction and post-construction settlements of the A2, A3, and A4 zones are shown in Table 2. It can be observed that the surface coral sand undergoes further compression and consolidation because of particle breakage and rearrangement after the vibro-flotation and impact rolling treatments. Specifically, the settlement ranges from 21.0 to 24.1 cm for the vibro-flotation treatment and from 19.5 to 21.6 cm for the impact rolling treatment. In conjunction with the post-treatment settlement analysis, it is found that the post-vibro-flotation treatment settlement after 30 days ranges from 3.5 to 5.1 mm, and the post-impact rolling treatment settlement ranges from 5.2 to 6.8 mm. Both treatments result in a very low post-treatment settlement, indicating a more stable state; moreover, those values are much lower than the allowable post-construction settlement for an airport runway, which is 0.2–0.3 m [34]. The results also coincide with the findings by Wang et al. [4] that the ground settlement of the hydraulic filling coral sand treated using vibroflotation tends to be stable after 21 days, and the average settlement is 4.3 mm after 61 days. This might be due to the relatively low compressibility of coral sand compared to quartz sand at low stress levels [12].

**Table 2.** Settlement observation results of each test point.

| Experimental Zone | Construction Settlement (cm) | | | Post-Construction Settlement after 30 Days (mm) | | |
|---|---|---|---|---|---|---|
| | Point 1 | Point 2 | Point 3 | Point 1 | Point 2 | Point 3 |
| A2 | 23.7 | 21.2 | 21.0 | 5.1 | 4.7 | 4.2 |
| A3 | 23.6 | 22.9 | 24.1 | 3.5 | 4.3 | 3.6 |
| A4 | 19.5 | 20.3 | 21.6 | 5.2 | 6.8 | 5.5 |

## 6. Conclusions

Through a series of on-site evaluation tests, this study examined the reinforcement effectiveness of various foundation treatment processes on a reclaimed coral sand foundation, considering aspects including the bearing capacity, deformation modulus, modulus of the subgrade reaction, CBR, DPT value, and settlement. The main findings are as follows:

(1) The untreated hydraulic-filled coral sand foundation exhibits a bearing capacity exceeding 150 kPa and a deformation modulus of 20 MPa. This high-bearing capacity and deformation modulus could satisfy the requirements of some light buildings and structures. After impact rolling treatment, the bearing capacity increases to larger than 300 kPa, and the deformation modulus reaches 40 MPa. Vibro-flotation could result in a slightly higher bearing capacity and deformation modulus than when using the impact rolling treatment. Since both treatment methods could make the bearing capacity of the foundation meet the maximum requirement of design load (300 kPa),

impact rolling is considered to be the most efficient in this study because of the simple machinery and quick construction speed;

(2) Comparing the modulus of the subgrade reaction and CBR values of the coral sand foundation before and after the impact rolling treatment, the untreated foundation exhibits a modulus reaction of 40 $MN/m^3$ and CBR values exceeding 15%. These values are relatively higher compared to common terrestrial fill soils, indicating the beneficial effect of seepage densification in increasing the foundation's strength. After the impact rolling treatment, the modulus of the reaction and CBR values further increased. Impact rolling caused particle breakage and rearrangement in the surface layer of the coral sand, enhancing compaction and deformation resistance. The finer particles filling the voids result in a greater interlocking effect, improving the strength and stability of the foundation to meet airport engineering design standards. Vibro-flotation could result in a slightly higher modulus of reaction and CBR values than the impact rolling treatment;

(3) Due to the high permeability resulting in rapid self-weight consolidation, the untreated coral sand foundation exhibits a relatively high degree of compaction. After impact rolling or vibro-flotation treatment, coral sand particles undergo breakage and rearrangement, leading to denser structures. The compaction degrees after treatment essentially meet the technical requirements for airport runways;

(4) The $N_{63.5}$ obtained from the DPT of the untreated coral sand foundation ranges from 5 to 12 within 6 m of depth, with the maximum value found at a depth of 1.5–2.0 m. After impact rolling or vibro-flotation treatment, the $N_{63.5}$ increases markedly. The most pronounced increase in $N_{63.5}$ occurs after vibro-flotation at a depth of 1–3 m. However, for foundation depths exceeding 3 m, the increase in $N_{63.5}$ is considerably less, suggesting that the reinforcement effect of both vibro-flotation and impact rolling on the deep foundation is not as substantial as in the surface layers;

(5) The untreated coral sand foundation, due to the effects of seepage densification and self-weight consolidation, experiences settlement during the drainage process. The consolidation occurs rapidly, with the foundation essentially stabilizing after one month, resulting in total settlements ranging from 27.5 to 32.8 cm. After impact rolling or vibro-flotation treatment, the foundation is further densified, with post-construction settlements ranging from 3.5 to 6.8 mm, indicating a more stable state.

**Author Contributions:** Conceptualization, T.Y. and W.L.; Methodology, W.L.; Formal analysis, T.Y. and W.L.; Investigation, T.Y.; Writing—original draft, T.Y. and W.L. All authors have read and agreed to the published version of the manuscript.

**Funding:** This research was funded by the National Key Technologies R&D Program of China [2022YFC3102101], the National Natural Science Foundation of China [42177154, 42102327, 42377176] and the Open Fund of the Key Laboratory of Special Environment Road Engineering of Hunan Province, Changsha University of Science & Technology, China [kfj220503]. The APC was funded by [42177154].

**Institutional Review Board Statement:** Not applicable.

**Informed Consent Statement:** Not applicable.

**Data Availability Statement:** The data presented in this study are available on request from the corresponding author.

**Conflicts of Interest:** The authors declare no conflict of interest.

## References

1. Darwin, C. *The Structure and Distribution of Coral Reefs*; Smith, Elder and Co.: London, UK, 1842.
2. Wang, X.; Weng, Y.; Wei, H.; Meng, Q.; Hu, M. Particle obstruction and crushing of dredged calcareous soil in the Nansha Islands, South China Sea. *Eng. Geol.* **2019**, *261*, 105274. [CrossRef]
3. Shen, J.H.; Wang, X.; Cui, J.; Wang, X.Z.; Zhu, C.Q. Shear characteristics of calcareous gravelly sand considering particle breakage. *Bull. Eng. Geol. Environ.* **2022**, *81*, 130. [CrossRef]

4. Wang, X.; Ding, H.; Wen, D.; Wang, X. Vibroflotation method to improve silt interlayers of dredged coral sand ground–a case study. *Bull. Eng. Geol. Environ.* **2022**, *81*, 472. [CrossRef]
5. Coop, C.A. Origin of carbonate sand. *Sedimentology* **1990**, *37*, 503–515.
6. Kong, D.; Fonseca, J. Quantification of the morphology of shelly carbonate sands using 3D images. *Géotechnique* **2018**, *68*, 249–261. [CrossRef]
7. Zhou, B.; Ku, Q.; Wang, H.; Wang, J. Particle classification and intra-particle pore structure of carbonate sands. *Eng. Geol.* **2020**, *279*, 105889. [CrossRef]
8. Wu, Y.; Li, N.; Wang, X.; Cui, J.; Chen, Y.; Wu, Y.; Yamamoto, H. Experimental investigation on mechanical behavior and particle crushing of calcareous sand retrieved from South China Sea. *Eng. Geol.* **2021**, *280*, 105932. [CrossRef]
9. Coop, M.R. The mechanics of uncemented carbonate sands. *Géotechnique* **1990**, *40*, 607–626. [CrossRef]
10. Wang, X.; Cui, J.; Wu, Y.; Zhu, C.; Wang, X. Mechanical properties of calcareous silts in a hydraulic fill island-reef. *Mar. Georesources Geotechnol.* **2021**, *39*, 1–14. [CrossRef]
11. Gao, R.; Ye, J. Mechanical behaviors of coral sand and relationship between particle breakage and plastic work. *Eng. Geo.* **2023**, *316*, 107063. [CrossRef]
12. Yao, T.; Li, W. Effect of initial fabric from sample preparation on the mechanical behaviour of a carbonate sand from the South China Sea. *Eng. Geol.* **2023**, *326*, 107311. [CrossRef]
13. Yao, T.; Li, W. Quantifying the particle shape and surface roughness of sands. *Bull. Eng. Geol. Environ.* **2023**, *82*, 135. [CrossRef]
14. Van't Hoff, J.; van der Kolff, A.N. *Hydraulic Fill Manual for Dredging and Reclamation Works*; CRC Press, Taylor and Francis Group: Boca Raton, FL, USA, 2012.
15. Dong, Y.; Wang, D.; Randolph, M.F. Quantification of impact forces on fixed mudmats from submarine landslides using the material point method. *Appl. Ocean Res.* **2020**, *102*, 102227. [CrossRef]
16. Fan, N.; Jiang, J.; Nian, T.; Dong, Y.; Guo, L.; Fu, C.; Tian, Z.; Guo, X. Impact action of submarine slides on pipelines: A review of the state-of-the-art since 2008. *Ocean Eng.* **2023**, *286*, 115532. [CrossRef]
17. Wang, X.; Ding, H.; Meng, Q.; Wei, H.; Wu, Y.; Zhang, Y. Engineering characteristics of coral reef and site assessment of hydraulic reclamation in the South China Sea. *Constr. Build. Mater.* **2021**, *300*, 124263. [CrossRef]
18. Chen, Y.; Jaksa, M.B.; Kuo, Y.L.; Airey, D.W. Experimental analysis of rolling dynamic compaction using transparent soils and particle image velocimetry. *Can. Geotech. J.* **2022**, *59*, 254–271. [CrossRef]
19. Ranasinghe, R.A.T.M.; Jaksa, M.B.; Pooya Nejad, F.; Kuo, Y.L. Predicting the effectiveness of rolling dynamic compaction using genetic programming. *Proc. Inst. Civ. Eng.-Ground Improv.* **2017**, *170*, 193–207. [CrossRef]
20. Xiao, Y.; Liu, H.; Chen, Q.; Long, L.; Xiang, J. Evolution of particle breakage and volumetric deformation of binary granular soils under impact load. *Granul. Matter* **2017**, *19*, 71. [CrossRef]
21. Xiao, Y.; Yuan, Z.; Chu, J.; Liu, H.; Huang, J.; Luo, S.N.; Wang, S.; Lin, J. Particle breakage and energy dissipation of carbonate sands under quasi-static and dynamic compression. *Acta Geotech.* **2019**, *14*, 1741–1755. [CrossRef]
22. Ke, J.; Ma, L.; Luo, Z.; Shi, X.; Song, Y.; Tan, Y. Compressibility and crushing of coral sands under one-dimensional dynamic compaction. *Granul. Matter* **2021**, *23*, 95. [CrossRef]
23. Van Impe, P.O.; Van Impe, W.F.; Manzotti, A.; Mengé, P.; Van den Broeck, M.; Vinck, K. Compaction control and related stress-strain behaviour of off-shore land reclamations with calcareous sands. *Soils Found.* **2015**, *55*, 1474–1486. [CrossRef]
24. Giretti, D.; Fioravante, V.; Been, K.; Dickenson, S. Mechanical properties of a carbonate sand from a dredged hydraulic fill. *Géotechnique* **2018**, *68*, 410–420. [CrossRef]
25. Giretti, D.; Been, K.; Fioravante, V.; Dickenson, S. CPT calibration and analysis for a carbonate sand. *Géotechnique* **2018**, *68*, 345–357. [CrossRef]
26. Wang, X.Z. Study on Engineering Geological Properties of Coral Reefs and Feasibility of Large Project Construction on Nansha Islands. Ph.D. Thesis, Institute of Rock and Soil Mechanics, The Chinese Academy of Sciences, Wuhan, China, 2008.
27. Sun, Z.; Zhan, W.; Zhu, J. Rockmass structure and engineering geological zones of coral reefs, Nansha Islands of South China Sea. *J. Trop. Oceanogr.* **2004**, *23*, 11–20.
28. *ASTM. D2487*; Standard Practice for Classification of Soils for Engineering Purposes (Unified Soil Classification System). American Society for Testing and Materials: West Conshohocken, PA, USA, 2017.
29. *ASTM. D4254-16*; Standard Test Methods for Minimum Index Density and Unit Weight of Soils and Calculation of Relative Density. American Society for Testing and Materials: West Conshohocken, PA, USA, 2016.
30. Lunne, T.; Knudsen, S.; Blaker, Ø.; Vestgården, T.; Powell, J.J.M.; Wallace, C.F.; Krogh, L.; Thomsen, N.V.; Yetginer, G.; Ghanekar, R.K. Methods used to determine maximum and minimum dry unit weights of sand: Is there a need for a new standard? *Can. Geotech. J.* **2019**, *56*, 536–553. [CrossRef]
31. *GB 50007-2011*; Code for Design of Building Foundation. National Standard of the People's Republic of China: Beijing, China, 2011.
32. Reznik, Y.M. Comparison of results of oedometer and plate load tests performed on collapsible soils. *Eng. Geol.* **1995**, *39*, 17–30. [CrossRef]
33. He, H.; Li, W.; Senetakis, K. Small strain dynamic behavior of two types of carbonate sands. *Soils Found.* **2019**, *59*, 571–585. [CrossRef]
34. *MH/T 5027-2013*; Code for Geotechnical Engineering Design of Airport. China Civil Aviation Press: Beijing, China, 2013.

35. *JTG 3450-2019*; Field Test Methods of Highway Subgrade and Pavement. Standard of the Ministry of Transport of the People's Republic of China: Beijing, China, 2019.
36. *GB 50021-2001*; Code for Investigation of Geotechnical Engineering. National Standard of the People's Republic of China: Beijing, China, 2009.
37. Wang, X.Z.; Wang, R.; Meng, Q.S.; Liu, X.P. Study of plate load test of calcareous sand. *Rock. Soil. Mech.* **2009**, *30*, 147–152.
38. Wang, X.Z.; Wang, X.; Liu, H.F.; Meng, Q.S.; Zhu, C.Q. Field test study of engineering behaviors of coral reef foundation. *Rock. Soil. Mech.* **2017**, *38*, 2065–2070.
39. *AASHTO T 193*; Standard Method of Test for the California Bearing Ratio. American Association of State Highway and Transportation Officials: Washington, DC, USA, 2022.
40. Hu, M.J.; Jiang, H.H.; Zhu, C.Q.; Weng, Y.L.; Ruan, Y.; Chen, W.J. Discussion on permeability of calcareous sand and its influencing factors. *Rock. Soil. Mech.* **2017**, *38*, 2895–2900.
41. Wang, X.Z.; Wang, X.; Chen, J.W.; Wang, R.; Hu, M.J.; Meng, Q.S. Experimental study on permeability characteristics of calcareous soil. *Bull. Eng. Geol. Environ.* **2018**, *77*, 1753–1762. [CrossRef]
42. Dong, Y.; Liu, C.; Wei, H.; Meng, Q.; Zhou, H. Size segregation mechanism of reclamation fill sand due to rainbowing operations in hydraulic dredging activities. *Ocean Eng.* **2021**, *242*, 109957. [CrossRef]